Proceedings of the 2000 IEEE
International Conference on Robotics & Automation
San Francisco, CA • April 2000

The Augmented Object Model: Cooperative Manipulation and Parallel Mechanism Dynamics

Kyong-Sok Chang, Robert Holmberg*, and Oussama Khatib

Robotics Laboratory, Computer Science Department
Stanford University, Stanford, CA 94305, U.S.A.
{kcchang, rah, ok}@robotics.stanford.edu

Abstract

The augmented object model provided the basis for effective cooperation between multiple robots. These robots were assumed to have a single serial-chain structure. In this paper we discuss the augmented object model in the context of mechanisms involving multiple branches such as humanoid robots and parallel mechanisms. An application of the proposed model in the dynamic modeling of a holonomic mobile base and experimental results using real-time dynamic simulation are presented to illustrate the effectiveness of the proposed approach.

1 Introduction

Cooperative manipulation is an important capability for extending the domain of robotic applications. It allows multiple robots to work together, resulting a significant increase in their overall effective workload and workspace. Various cooperation strategies have been proposed [14, 4, 10, 11, 1, 5]. Our earlier work on cooperative manipulation by multiple fixed-base serial-chain manipulators established the *augmented object model* describing the dynamics at the level of the manipulated object [7], and the *virtual linkage model* [13] characterizing internal forces.

This paper presents the extension and integration of these two basic models in order to accommodate the closed-chain dynamics of systems involving branching mechanisms (Figure 1) while preserving overall performance. The discussion in this paper focuses on the *augmented object model* as dynamic modeling of cooperative manipulation among multiple robotic platforms involving multiple branches and parallel mechanisms. This model, in conjunction with the virtual linkage model, naturally renders a cooperative control structure consistent with the operational space formulation. This control structure provides the effective object-level control of the closed-chain dynamics and the object internal forces.

Section 2 reviews the basics of the operational space formulation for branching robots and the task/posture behavior concept under this formulation. In section 3, we develop the augmented object model as dynamic modeling of closed-chain dynamics involving multiple branching robots. Also, an operational space dynamic control structure is developed using this model and the virtual linkage model. Section 4 presents, in detail, an application of the augmented object model in the dynamic modeling of a 4-wheel holonomic mobile base. Finally, real-time simulation results with a 24-degree-of-freedom humanoid robot are presented.

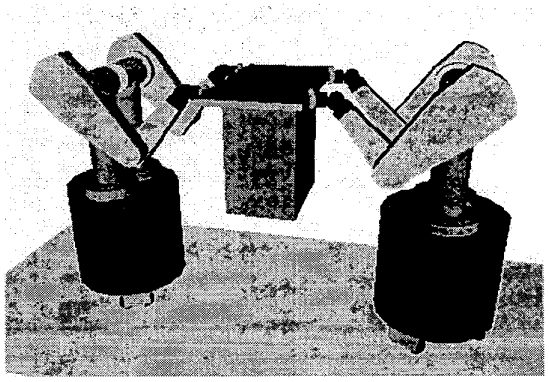

Figure 1: Cooperation by multiple branching robots

2 Operational Space Formulation

The *operational space formulation* [6, 9] for a branching robot with multiple (m) operational points (end-effectors) provides dynamic modeling and control directly in the operational space by projecting the joint

*Department of Mechanical Engineering

space dynamics into the operational space and its associated null space. The general joint space dynamic equations of motion for an open-chain branching robotic mechanism can be written as [12]:

$$\mathbf{A}\,\ddot{\mathbf{q}} + \mathbf{b} + \mathbf{g} = \tau \tag{1}$$

where $\mathbf{A}$ is the joint space inertia matrix. $\ddot{\mathbf{q}}$, $\mathbf{b}$, $\mathbf{g}$, and τ are the joint space acceleration, Coriolis and centrifugal force, gravitational force, and total control torque vectors, respectively.

The generalized torque/force relationship [6, 9] in the operational space formulation provides a decomposition of the total control torque, τ in Equation (1) into two dynamically decoupled control torque vectors: the torque corresponding to the task behavior command vector and the torque that only affects posture behavior in the null space:

$$\tau = \tau_{task} + \tau_{posture} \tag{2}$$

It is critical for the end-effectors to maintain their responsiveness and to be dynamically decoupled from the posture behavior. The posture can then be treated separately from the end-effectors' tasks, allowing intuitive task specifications and effective robot control.

2.1 Task Behavior

τ_{task} in Equation (2) is the torque corresponding to the computed task behavior command vector, $\mathbf{f}$, acting in the operational space:

$$\tau_{task} = \mathbf{J}^T \mathbf{f} \tag{3}$$

where $\mathbf{f}$ is a vertically concatenated vector of the force vector of each of m end-effectors and $\mathbf{J}$ is the vertically concatenated matrix of the Jacobian matrix of each of m end-effectors:

$$\mathbf{f} = \begin{bmatrix} \mathbf{f}_{e_1} \\ \vdots \\ \mathbf{f}_{e_m} \end{bmatrix} \quad \text{and} \quad \mathbf{J} = \begin{bmatrix} \mathbf{J}_{e_1} \\ \vdots \\ \mathbf{J}_{e_m} \end{bmatrix} \tag{4}$$

Since dynamic control of task behavior in the operational space is desired, $\mathbf{f}$ can be computed using the operational space (task behavior) command vector for a linearized unit-mass system, $\ddot{\mathbf{x}}$, and the dynamics obtained by projecting the joint space dynamics into its operational space:

$$\Lambda\,\ddot{\mathbf{x}} + \mu + \mathbf{p} = \mathbf{f} \tag{5}$$

where the operational space inertia matrix, Λ, is a symmetric positive definite matrix [6, 9]:

$$\Lambda^{-1} = \mathbf{J}\,\mathbf{A}^{-1}\,\mathbf{J}^T \tag{6}$$

and $\mathbf{p}$ and μ are the operational space gravitational force and Coriolis and centrifugal force vectors, respectively. $\bar{\mathbf{J}}$ is the dynamically consistent generalized inverse of the Jacobian matrix $\mathbf{J}$ in Equation (4) and has been proven to be unique [6, 9]:

$$\bar{\mathbf{J}}^T = \Lambda\,\mathbf{J}\,\mathbf{A}^{-1} \tag{7}$$

2.2 Posture Behavior

τ_{task} in Equation (2) is the torque that only affects posture behavior in the null space given any arbitrary null space (posture behavior) command vector, τ_{null}:

$$\tau_{posture} = \mathbf{N}^T \tau_{null} \tag{8}$$

where $\mathbf{N}$ is the dynamically consistent null space projection matrix that maps $\tau_{posture}$ to the appropriate control torque:

$$\mathbf{N} = \mathbf{I} - \bar{\mathbf{J}}\,\mathbf{J} \tag{9}$$

where $\mathbf{I}$ is an identity matrix.

Dynamic consistency is the essential property for task behavior to maintain its responsiveness and to be dynamically decoupled from posture behavior since it guarantees not to produce any coupling acceleration in the operational space given any τ_{null}. In Figure 2, the robot was commanded to keep the position of both hands constant (task behavior) while rocking its torso back and forth in the null space (posture behavior). Notice that dynamic consistency enables task behavior and posture behavior to be specified independently of each other, providing an intuitive control of complex systems.

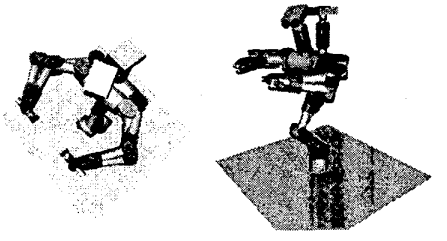

Figure 2: Posture behavior

3 Cooperative Manipulation

Our approach is based on the extension and integration of two basic concepts: The *augmented object* [7] and the *virtual linkage* [13]. The *virtual linkage* characterizes internal forces, while the *augmented object* describes the system's closed-chain dynamics.

First we will present object-level modeling of closed-chain dynamics involving branching robots. The corresponding cooperation control strategy will be presented in a subsequent section.

3.1 Augmented Object Model

The earlier *augmented object model* [7] provides a description of the dynamics at the operational point for a multi-manipulator system, where each manipulator has a stationary base fixed in a common inertial frame. In this subsection, we present the augmented object model to accommodate branching systems, where all of the manipulators in the systems are cross-coupled not only through the object but also through their common links.

The equations of motion of a closed-chain system under the *augmented object model* can be written as:

$$\mathbf{\Lambda}_{\oplus}\,\ddot{\mathbf{x}}_{obj} + \boldsymbol{\mu}_{\oplus} + \mathbf{p}_{\oplus} = \mathbf{f}_{\oplus} \tag{10}$$

where $\mathbf{x}_{obj}$ is the operational space coordinates of the object. $\mathbf{\Lambda}_{\oplus}$, $\boldsymbol{\mu}_{\oplus}$, and $\mathbf{p}_{\oplus}$ are the kinetic energy matrix (operational space inertia matrix), the centrifugal and Coriolis force vector, and the gravity vector associated with the system of an object and branching robots, respectively. The generalized operational force vector, $\mathbf{f}_{\oplus}$, is the resultant of the forces produced by all end-effectors at the operational point.

The simplicity of the equations associated with this model is the result of an additive property that allows us to obtain the system equations of motion from the the dynamics of the individual branching mechanisms.

3.1.1 For Single Branching Robot

This section develops the *augmented object model* from Equation (10) for branching robots (Figure 3).

This model formulates the simple closed-chain dynamics as an object-level dynamics with grasping constraint forces using the operational space formulation without modifying underlying kinematic and dynamic structures such as the Jacobian matrix. Therefore, this model renders an object-level operational space formulation to solve the dynamics of the simple closed-chain involving a branching mechanism.

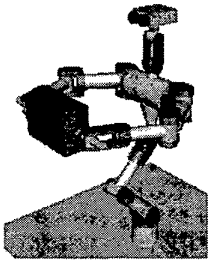

Figure 3: A branching robot holding an object

The kinetic energy matrix associated with a closed-chain system consisting of an object and a branching robot with m end-effectors can be written as:

$$\mathbf{\Lambda}_{\oplus} = \mathbf{\Lambda}_{obj} + \mathbf{C}^T\,\mathbf{\Lambda}\,\mathbf{C} \tag{11}$$

where $\mathbf{\Lambda}_{obj}$ and $\mathbf{\Lambda}$ are the kinetic energy matrices associated with the object and the open-chain branching robot, respectively. $\mathbf{C}$ represents the connectivity of m end-effectors to the common object. This matrix is the vertically concatenated matrix of m identity matrices for a simple closed-chain:

$$\mathbf{C} = [\mathbf{I}_i \cdots \mathbf{I}_m]^T \tag{12}$$

Equation (11) results from the evaluation of the total kinetic energy, KE, of the closed-chain system expressed with respect to the operational space velocities:

$$KE = \frac{1}{2}\dot{\mathbf{x}}_{obj}^T\,\mathbf{\Lambda}_{\oplus}\,\dot{\mathbf{x}}_{obj} = \frac{1}{2}\dot{\mathbf{x}}_{obj}^T\,\mathbf{\Lambda}_{obj}\,\dot{\mathbf{x}}_{obj} + \frac{1}{2}\dot{\mathbf{x}}^T\,\mathbf{\Lambda}\,\dot{\mathbf{x}}$$

where $\dot{\mathbf{x}}$ is the operational space velocity vector of m end-effectors of a branching robot and can be written as:

$$\dot{\mathbf{x}} = \mathbf{C}\,\dot{\mathbf{x}}_{obj}$$

since the object and all end-effectors are expressed at the same operational point with the rigid grasp assumption.

The centrifugal and Coriolis vector of the closed-chain system, $\boldsymbol{\mu}_{\oplus}$, has the additive property:

$$\boldsymbol{\mu}_{\oplus} = \boldsymbol{\mu}_{obj} + \mathbf{C}^T\,\boldsymbol{\mu} \tag{13}$$

where $\boldsymbol{\mu}_{obj}$ and $\boldsymbol{\mu}$ are the vectors of centrifugal and Coriolis forces associated with the object and the open-chain branching robot, respectively. Similarly, the gravity vector of the closed-chain system, $\mathbf{p}_{\oplus}$, can be written as:

$$\mathbf{p}_{\oplus} = \mathbf{p}_{obj} + \mathbf{C}^T\,\mathbf{p} \tag{14}$$

where $\mathbf{p}_{obj}$ and $\mathbf{p}$ are the gravity vectors associated with the object and the open-chain branching robot, respectively.

3.1.2 For Multiple Branching Robots

When N branching robots grasp the same common object (Figure 1), Equation (10) still holds and the operational space dynamics of the system simply become the sum of the operational space dynamics of the object and each branching robot, all expressed at the same operational point.

Since the rigid grasp is assumed, the operational space velocity of the end-effectors of i^{th} branching robot can be written as:

$$\dot{\mathbf{x}}_i = \mathbf{C}_i \, \dot{\mathbf{x}}_{obj} \tag{15}$$

where $\mathbf{C}_i$ represents the connectivity of the end-effectors of the i^{th} branching robot to the common object for a simple closed-chain. Then, the augmented object model for the closed-chain dynamics of the system consisting of a common object and multiple (N) branching robots can be written as:

$$\mathbf{\Lambda}_{\oplus} = \mathbf{\Lambda}_{obj} + \sum_{i=1,\ldots,N} \mathbf{C}_i^T \, \mathbf{\Lambda}_i \, \mathbf{C}_i \tag{16}$$

$$\boldsymbol{\mu}_{\oplus} = \boldsymbol{\mu}_{obj} + \sum_{i=1,\ldots,N} \mathbf{C}_i^T \, \boldsymbol{\mu}_i \tag{17}$$

$$\mathbf{p}_{\oplus} = \mathbf{p}_{obj} + \sum_{i=1,\ldots,N} \mathbf{C}_i^T \, \mathbf{p}_i \tag{18}$$

where $\mathbf{\Lambda}_i$, $\boldsymbol{\mu}_i$, and $\mathbf{p}_i$ represent the operational space dynamic components of the i^{th} branching robot.

3.2 Dynamic Control

3.2.1 Virtual Linkage Model

Object manipulation requires accurate control of internal forces. we have proposed the *virtual linkage* [13], as a model of object internal forces associated with multi-grasp manipulation. In this model, grasp points are connected by a closed, non-intersecting set of virtual links. Compared to other methods used to characterize internal forces, the virtual linkage model has the advantage of providing a physical representation of internal forces and moments. This allows control of non-zero internal forces to have a physically meaningful effect on the manipulated object.

3.2.2 Operational Space Control Structure

The dynamically consistent generalized inverse of the Jacobian matrix, $\overline{\mathbf{J}}$ in Equation (7) has been proven to be load independent [3]. This immediately provides an important result; the dynamically consistent null space mapping matrix for the closed-chain system is the same as the one for the open-chain system, $\mathbf{N}$ in Equation (9). Therefore, we can control the closed-chain system with the same control structure in Equation (2) for the open-chain system except the operational space control force, $\mathbf{f}$ in Equation (5) should reflect the augmented object model and the virtual linkage model:

$$\mathbf{f} = \mathbf{G}^{-1} \begin{bmatrix} \mathbf{f}_{res} \\ \mathbf{f}_{int} \end{bmatrix} \tag{19}$$

where $\mathbf{f}_{res}$ is the resultant force at the operational point and is equivalent to $\mathbf{f}_{\oplus}$. $\mathbf{f}_{int}$ is the internal force and $\mathbf{G}$ is the grasp description matrix. The grasp description matrix contains a model of the internal force representation as well as the relationship between applied grasp forces and object resultant forces. Thus this matrix is central to the control scheme employed by the virtual linkage model. For the cooperative operations among multiple robots, a hybrid strategy of the *centralized* and *decentralized* control architecture [8] provides an effective implementation consistent with the augmented object and virtual linkage models, while preserving the overall performance of the system.

4 An Application

In this section, we present an application of the augmented object model in the dynamic modeling of a *powered caster vehicle* (PCV) such as the holonomic mobile base in Figure 4.

Figure 4: Nomadic XR4000 and PUMA 560

The use of a dynamically-controlled, holonomic mobile base in a mobile manipulation system is particularly desirable since it provides easier planning and navigation for gross motion, along with the ability to fully use the null space motions of the system to improve the workspace and overall dynamic properties.

Typically, the dynamic equations of motion for a parallel system with non-holonomic constraints such as a PCV are formed in one of two ways: the unconstrained dynamics of the whole system is derived and the the constraints are applied to reduce the number of degrees of freedom [2]; or the system is cut up into pieces, the dynamics of these subsystems are computed, and the loop closure equations are used to eliminate the extra degrees of freedom.

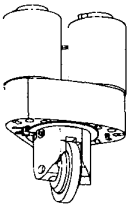

Figure 5: Powered caster module

For the Nomadic XR4000 robot in Figure 4, a mobile base with four powered caster modules (Figure 5), the first method generates 11 equations for the unconstrained system and 8 constraint equations. The second method generates 12 equations for the unconstrained subsystems and 9 constraint equa-

tions. These systems of equations must then be reduced to 3 equations. Ideally, both these methods would yield the same minimal set of dynamic equations, but in practice it is difficult to reduce the proliferation of terms that are introduced in such a large number of equations.

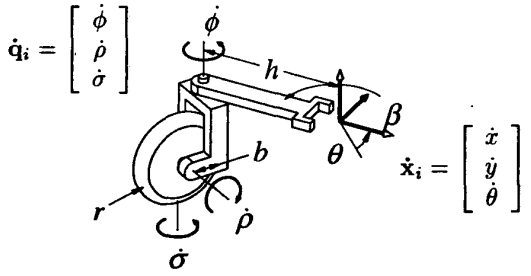

Figure 6: A 3-DOF serial manipulator

In order to get a more efficient set of dynamic equations of motion we will use a method which uses compatible 3-degree-of-freedom (DOF) systems since each powered caster module of the PCV (Figure 5) can be modeled as a 3-DOF serial manipulator shown in Figure 6. In this figure, $\dot{\phi}$ is the steering rate, $\dot{\rho}$ is the angular speed of rolling, and $\dot{\sigma}$ is the angular twist rate at the wheel contact. $\dot{\mathbf{x}}_i$ is the operational space velocity vector of the i^{th} manipulator. Then, the dynamics of the PCV can be modeled as the cooperative manipulation of these 3-DOF manipulators.

Similarly to Equation (1), the joint space equations of motion of the i^{th} 3-DOF serial manipulator can be written:

$$\mathbf{A}_i \ddot{\mathbf{q}}_i + \mathbf{b}_i = \boldsymbol{\tau}_i \tag{20}$$

Note that there is no effect of gravity since the PCV is assumed to be on level ground.

Since this manipulator is non-redundant, the inverse of the Jacobian matrix, $\mathbf{J}^{-1}$, is computed directly for the computational efficiency:

$$\dot{\mathbf{q}}_i = \mathbf{J}_i^{-1} \dot{\mathbf{x}}_i \tag{21}$$

$$\mathbf{J}_i^{-1} = \begin{bmatrix} -\mathrm{s}\phi/b & \mathrm{c}\phi/b & h[\mathrm{c}\beta\mathrm{c}\phi + \mathrm{s}\beta\mathrm{s}\phi]/b - 1 \\ \mathrm{c}\phi/r & \mathrm{s}\phi/r & h[\mathrm{c}\beta\mathrm{s}\phi - \mathrm{s}\beta\mathrm{c}\phi]/r \\ -\mathrm{s}\phi/b & \mathrm{c}\phi/b & h[\mathrm{c}\beta\mathrm{c}\phi + \mathrm{s}\beta\mathrm{s}\phi]/b \end{bmatrix}$$

where s· and c· are the shorthand for $\sin(\cdot)$ and $\cos(\cdot)$. It is interesting to note that the first two rows of $\mathbf{J}^{-1}$ express the non-holonomic constraints due to ideal rolling while the third row is a holonomic constraint: $\theta = \sigma - \phi$.

Using Equations (20) and (21), the operational space dynamics of the i^{th} manipulator can be written similarly to Equation (5):

$$\boldsymbol{\Lambda}_i \ddot{\mathbf{x}}_i + \boldsymbol{\mu}_i = \mathbf{f}_i \tag{22}$$

$$\boldsymbol{\Lambda}_i = \mathbf{J}_i^{-T} \mathbf{A}_i \mathbf{J}_i^{-1} \quad ; \quad \boldsymbol{\mu}_i = \mathbf{J}_i^{-T} \left(\mathbf{A}_i \dot{\mathbf{J}}_i^{-1} \dot{\mathbf{x}}_i + \mathbf{b}_i \right)$$

Note that $\boldsymbol{\mu}_i$ is expressed explicitly as a function of $\dot{\mathbf{x}}_i$ as well as $\mathbf{q}_i$ and $\dot{\mathbf{q}}_i$ in order to utilize the best estimates of the base velocity in addition to exact local information such as directly measured rolling speed of the wheel.

By assigning the end-effector frames of all manipulators such that they are coincident with the base (object) frame and using Equation (15), the operational space velocity of each manipulator is $\dot{\mathbf{x}}_i = \dot{\mathbf{x}}_{obj}$ since $\mathbf{C}_i$ in Equation (12) is an 3×3 identity matrix. Then, the operational space dynamic components from Equations (16), (17), and (18), can be written as:

$$\boldsymbol{\Lambda}_\oplus = \sum_i \boldsymbol{\Lambda}_i \quad ; \quad \boldsymbol{\mu}_\oplus = \sum_i \boldsymbol{\mu}_i \quad ; \quad \mathbf{f}_\oplus = \sum_i \mathbf{f}_i$$

where $\boldsymbol{\Lambda}_\oplus$, $\boldsymbol{\mu}_\oplus$, and $\mathbf{f}_\oplus$ represent the dynamic properties of the entire mobile base.

Finally, using these, the equations of motion of the PCV can be written as the equations of motion under the augmented object model from Equation (10):

$$\boldsymbol{\Lambda}_\oplus \ddot{\mathbf{x}}_{obj} + \boldsymbol{\mu}_\oplus = \mathbf{f}_\oplus \tag{23}$$

Notice that Equation (23) directly generates the required 3 operational space dynamic equations for the PCV. It does not generate terms which add and/or cancel as is the case with other methods. Using the symbolic dynamic equation generator AUTOLEV to create $\boldsymbol{\Lambda}_\oplus$ and $\boldsymbol{\mu}_\oplus$ for the Nomadic XR4000, the number of multiplies and additions are reduced from 8180 and 2244, to 2174 and 567, respectively, resulting a significant increase in computational efficiency.

5 Experimental Results

Using the methods presented in previous sections, we were able to perform the computation of the closed-chain dynamics under the operational space formulation for the humanoid robot in Figure 3 in less than 1.5 msec using a PC with a 266 MHz Pentium II running under the QNX real-time operating system. This branching robot has an operational point at each of its 2 end-effectors and 24 links connected by 1-DOF joints.

Figure 7 shows the motion sequence when this robot was commanded to put the box on the floor while being advised to keep its posture the same as the initial configuration. Notice that the robot had to adjust its advised posture behavior in the null space without producing any coupling acceleration at both end-

effectors in order not to violate the primary task behavior. This was done automatically without any additional commands.

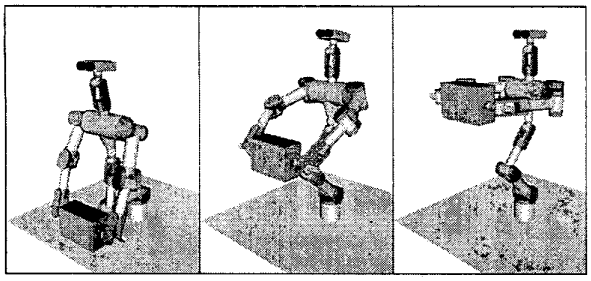

Figure 7: Sequence of putting a box on the floor

6 Conclusion

We have proposed the *augmented object model* as the dynamic modeling of effective cooperative manipulation among multiple robotic platforms involving multiple branches and holonomic or non-holonomic parallel mechanisms. The simplicity of the equations associated with this model is the result of an additive property that allows us to obtain the system equations of motion from the the dynamics of the individual branching mechanisms. An application of the proposed augmented object model in the dynamic modeling of a holonomic mobile base is presented in detail. The augmented object model, in conjunction with the virtual linkage model, naturally renders a cooperative control structure consistent with the operational space formulation. This control structure provides the effective object-level control of the closed-chain dynamics and the object internal forces. The real-time simulation results with a 24-DOF humanoid robot illustrate the effectiveness of the proposed approach.

Acknowledgments

Many thanks to Oliver Brock, Oscar Madrigal, Diego Ruspini, Luis Sentis, H.F. Machiel Van der Loos, and Kazuhito Yokoi for their comments and support during the preparation of this manuscript.

References

[1] J. Adams, R. Bajcsy, J. Kosecka, V. Kumar, R. Mandelbaum, M. Mintz, R. Paul, C. Wang, Y. Yamamoto, and X. Yun. Cooperative material handling by human and robotic agents: Module development and system synthesis. In *Proceedings of IEEE/RSJ International Conference on Intelligent Robots and Systems*, pages 200–205, 1995.

[2] G. Campion, G. Bastin, and B. d'Andréa-Novel. Structural properties and classification of kinematic and dynamic models of wheeled mobile robots. In *Proceedings of IEEE International Conference on Robotics and Automation*, pages 462–469, Atlanta, GA, U.S.A., May 1993.

[3] R. Featherstone and O. Khatib. Load independence of the dynamically consistent inverse of the jacobian matrix. *International Journal of Robotics Research*, 16(2):168–170, April 1997.

[4] S. Hayati. Hybrid position/force control of multi-arm cooperating robots. In *Proceedings of IEEE International Conference on Robotics and Automation*, pages 82–89, San Francisco, CA, U.S.A., April 1986.

[5] D. Jung, G. Cheng, and A. Zelinsky. Experiments in realizing cooperation between autonomous mobile robots. In *Proceedings of International Symposium on Experimental Robotics*, pages 513–524, 1997.

[6] O. Khatib. A unified approach to motion and force control of robot manipulators: The operational space formulation. *IEEE Journal of Robotics and Automation*, RA-3(1):43–53, February 1987.

[7] O. Khatib. Object manipulatin in a muti-effector robot system. In R. Bolles and B. Roth, editors, *Robotics Research*, volume 4, pages 137–144. MIT Press, 1988.

[8] O. Khatib, K. Yokoi, O. Brock, K.-S. Chang, and A. Casal. Robots in human environments: Basic autonomous capabilities. *International Journal of Robotics Research*, 18(7):684–696, 1999.

[9] J. Russakow, O. Khatib, and S. M. Rock. Extended operational space formulation for serial-to-parallel chain (branching) manipulators. In *Proceedings of IEEE International Conference on Robotics and Automation*, pages 1056–1061, Nagoya, Japan, May 1995.

[10] T.-J. Tarn, A. K. Bejczy, and X. Yun. Design of dynamic control of two cooperating robot arms: Closed chain formulation. In *Proceedings of IEEE International Conference on Robotics and Automation*, pages 7–13, April 1987.

[11] M. Uchiyama and P. Dauchez. A symmetric hybrid position/force control scheme for the coordination of two robots. In *Proceedings of IEEE International Conference on Robotics and Automation*, pages 350–356, April 1988.

[12] M. W. Walker and D. E. Orin. Efficient dynamic computer simulation of robotic mechanisms. *Transactions of ASME Journal of Dynamic Systems, Measurement, and Control*, 104(3):205–211, September 1982.

[13] D. Williams and O. Khatib. The virtual linkage: A model for internal forces in multi-grasp manipulation. In *Proceedings of IEEE International Conference on Robotics and Automation*, volume 1, pages 1025–1030, Atlanta, GA, U.S.A., May 1993.

[14] Y. F. Zheng and J. Y. S. Luh. Joint torques for control of two coordinated moving robots. In *Proceedings of IEEE International Conference on Robotics and Automation*, pages 1375–1380, April 1986.